



## Executive summary

# Embrittlement of Archaeological Silver and Iron



**Report no.**  
NLR-TP-2009-105

**Author(s)**  
R.J.H. Wanhill

**Report classification**  
UNCLASSIFIED

**Date**  
March 2009

**Knowledge area(s)**  
Material & Damage Research

**Descriptor(s)**  
archeometry  
silver  
iron  
embrittlement  
conservation

### **Problem area**

Embrittlement of originally ductile archaeological metals is a complex phenomenon. The analysis and characterization of embrittlement requires specialist metallurgical knowledge and techniques. Understanding the embrittlement is important for selecting the best measures for restoration and conservation.

### **Description**

Several ancient embrittled silver objects and an iron pile-shoe were investigated using a variety of diagnostic techniques. These techniques enabled the most probable mechanisms of embrittlement to be determined, leading to recommendations for preserving these and other embrittled objects against further damage.

This report has been prepared in the format required for submission to the journal Structural Integrity and Life, Belgrade, Serbia.





NLR-TP-2009-105

## Embrittlement of Archaeological Silver and Iron

R.J.H. Wanhill

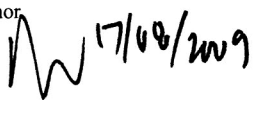
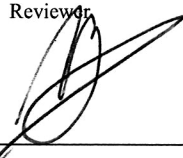
This report has been prepared in the format required for submission to the journal Structural Integrity and Life, Belgrade, Serbia.

The contents of this report may be cited on condition that full credit is given to NLR and the author.

This publication has been refereed by the Advisory Committee AEROSPACE VEHICLES.

Customer                      National Aerospace Laboratory NLR  
Contract number            ----  
Owner                         National Aerospace Laboratory NLR  
Division NLR                 Aerospace Vehicles  
Distribution                 Unlimited  
Classification of title        Unclassified  
                                      August 2009

Approved by:

Author  17/08/2009	Reviewer  18/8/09	Managing department  24/10/09
--	---	---





## **Summary**

Embrittlement of originally ductile archaeological metals is, or can be, a complex phenomenon. Some of the techniques required for the analysis and characterization of embrittlement were unavailable a generation ago and are not yet fully exploited by the archaeological community. It is important to understand the details and mechanisms of embrittlement in order to recommend and select the best remedial measures for restoration and conservation. This report presents a survey of the techniques used to investigate the embrittlement of several ancient embrittled silver objects and an iron pile-shoe from a Roman bridge. These techniques enabled the most probable mechanisms of embrittlement to be determined, leading to recommendations for preserving these and other embrittled objects against further damage.

## Contents

<i>Abstract</i>	5
<b>1. INTRODUCTION</b>	<b>5</b>
<b>2. ANCIENT SILVER EMBRITTLEMENT</b>	<b>5</b>
2.1 <i>Egyptian vase (Allard Pierson Museum, Amsterdam)</i>	5
2.2 <i>Gundestrup Cauldron (National Museum of Denmark, Copenhagen)</i>	6
2.3 <i>Byzantine paten (The Menil Collection, Houston)</i>	6
2.4 <i>Types of embrittlement and their severity</i>	6
2.5 <i>Corrosion damage, retained cold-work and discontinuous precipitation</i>	7
2.6 <i>Survey of diagnostic techniques</i>	7
2.7 <i>Remedial measures</i>	7
<b>3. ROMAN PILE-SHOE EMBRITTLEMENT</b>	<b>8</b>
3.1 <i>The collaborative investigation</i>	8
3.2 <i>Embrittlement mechanisms</i>	8
3.3 <i>Conservation of other pile-shoes</i>	9
<b>4. CONCLUDING REMARKS</b>	<b>9</b>
<b>5. ACKNOWLEDGEMENTS</b>	<b>9</b>
<b>6. REFERENCES</b>	<b>9</b>

Russell Wanhill<sup>1</sup>

## EMBRITTLLEMENT OF ARCHAEOLOGICAL SILVER AND IRON

Author's address:

<sup>1</sup>) National Aerospace Laboratory NLR, Amsterdam, the Netherlands

[wanhill@nlr.nl](mailto:wanhill@nlr.nl)

### Keywords

- archaeometry
- silver
- iron
- embrittlement
- conservation

### Abstract

Embrittlement of originally ductile archaeological metals is, or can be, a complex phenomenon. It is important to understand the details and mechanisms of embrittlement in order to recommend and select the best remedial measures for restoration and conservation. This paper presents a survey of the techniques used to investigate the embrittlement of several ancient embrittled silver objects and an iron pile-shoe from a Roman bridge. These techniques enabled the most probable mechanisms of embrittlement to be determined, leading to recommendations for preserving these and other embrittled objects against further damage.

## 1. INTRODUCTION

Several embrittled silver objects with widely varying provenance have been investigated by the NLR since 1994. These are an Egyptian vase, the Gundestrup Cauldron and a Byzantine paten (a plate used during celebration of the Eucharist). Also, a recent brittle fracture in a Roman pile-shoe recovered from the Maas riverbed in 1992 was investigated in collaboration with three other institutes in the Netherlands. The experience gained from these studies has enabled the most probable mechanisms of embrittlement to be determined, leading to recommendations for preserving these and other similarly embrittled objects against further damage, /1–7/.

Some of the techniques required for these studies were unavailable a generation ago and are not yet fully exploited by the archaeological community. This paper presents a survey of all the techniques used, and discusses their diagnostic capabilities.

## 2. ANCIENT SILVER EMBRITTLLEMENT

### 2.1 Egyptian vase (Allard Pierson Museum, Amsterdam)

Figure 1 shows the Egyptian vase, which is from the Ptolemaic period and dated to between 300 and 200 BCE. The vase is decorated with chased and stamped representations of flowers and lotus and acanthus leaves. The X-ray radiograph in figure 2 shows that the vase has been much restored (this is an old restoration, done in the late 19th Century). Figure 2 also reveals cracks following external chasing grooves and criss-crossing in a brittle “eggshell” crack pattern.

Small samples from the lip and lower wall of the vase were subjected to Scanning Electron Microscope (SEM) + Energy Dispersive analysis of X-rays (EDX) chemical analysis; SEM Secondary Electron (SE) and BackScattered Electron (BSE) metallography and fractography; and microhardness testing, /1/.

The EDX analyses gave the following average chemical composition, in wt.%: Ag 97.1. Au 0.8; Cu 0.9; Pb 0.7; Bi 0; Sn 0.2; Sb 0.3. Figures 3–6 illustrate some of the SEM results. The vase proved to be archetypal for:

- Corrosion-induced embrittlement along slip lines, deformation twin boundaries and segregation bands.
- Microstructurally-induced embrittlement, whereby the vase's chemical composition (0.7 % Pb, no Bi) indicates lead to be the most likely perpetrator, /1–4, 8/.
- Synergistic embrittlement.
- A link between retained cold-work and corrosion damage.

Figure 6 illustrates an especially significant link between retained cold-work and corrosion. The BSE imaging revealed a local deformation pattern. The adjacent schematic interprets this deformation pattern from the slip-line field theory of indentation, /9/. Besides the compression zone, this theory predicts that when  $t_i/w = 4.4$  a tension zone forms from the surface opposite the indentation: the actual value of  $t_i/w$  is 4.2, which is close enough to justify the interpretation. The significant point is that the tension zone promoted corrosion and intergranular fracture at and near the *internal surface* of the vase, i.e. it caused "hidden" damage.

## 2.2 Gundestrup Cauldron (National Museum of Denmark, Copenhagen)

Figure 7 shows the reassembled Gundestrup Cauldron, which is the largest surviving silverwork object from the European Iron Age, dating to the 2nd or 1st century BCE. Owing to its size, high quality workmanship and iconographic variety, the Cauldron has been the subject of many studies, particularly its origin, which is still controversial. The Cauldron consists of twelve plates and a bowl, all of 95–98 % silver. Chemical analyses showed copper to be the main alloying (or impurity) element, /10–11/.

Four small metallographic samples from different parts of the Cauldron were lent to the NLR by Peter Northover, Oxford University. The samples were examined using a Field Emission Gun Scanning Electron Microscope (FEG-SEM) combined with automated Electron BackScatter Diffraction (EBSD) equipment. EBSD is a powerful technique for microstructural analysis, providing many options. For the Gundestrup Cauldron samples the following options were found to be of most use, /12/:

- Inverse Pole Figure (IPF) colour-coded maps.
- Boundary rotation angle maps.
- Coincidence Site Lattice (CSL) maps.

Figures 8–12 illustrate the EBSD analysis results, which fall into two categories:

- (1) *Sample 366*: This sample was essentially annealed and virtually free of corrosion. The most significant results were a random microtexture, figure 8a, and extensive grain boundary precipitation of copper, giving the grain boundaries a meandering appearance, as in figure 8b. The details in figure 9 prove it to be discontinuous precipitation, /13–15/.
- (2) *Samples 361, 363, 365*: These samples contained increasing amounts of retained cold-work and corrosion damage. In figures 10–12 the retained cold-work is visible as red regions (slip) and irregular yellow boundaries (deformation twins). The corrosion damage is visible as black regions, representing mainly intergranular cracks but also transcrystalline cracks (best seen in figure 12a). However, there was no evidence of discontinuous precipitation.

## 2.3 Byzantine paten (The Menil Collection, Houston)

Figure 13 shows the Byzantine paten, which has been dated to about 600 AD. The paten is a rare and high-quality liturgical altar object. The important central tableau is well preserved, but there has been extensive breakage along the surrounding circular decorating grooves.

A small sample from the paten was examined by SEM metallography and EDX in a preliminary investigation at the Netherlands Institute for Cultural Heritage (ICN) in Amsterdam. Figure 14 illustrates the results. The sample showed surficial (shallow) intergranular corrosion, figure 14a, and at higher magnifications discontinuous precipitation of copper at the grain boundaries, figure 14b. This precipitation gave the grain boundaries a meandering appearance similar to that in figure 8b.

## 2.4 Types of embrittlement and their severity

Of the three types of embrittlement, corrosion-induced, microstructurally-induced, and synergistic, corrosion-induced embrittlement is much more common, /3–4/, and its severity varies

widely. Preliminary examination of a Roman kantharos (a highly ornamented beaker), /19/, indicates that microstructurally-induced embrittlement can be severe, but it seems to be much rarer. This is just as well, since its synergistic combination with corrosion is very detrimental, rendering an object not only frangible but friable. Special care should be taken to conserve such objects, /1/.

### 2.5 Corrosion damage, retained cold-work and discontinuous precipitation

On balance, and especially in view of the Gundestrup Cauldron results, it appears that retained cold-work is generally responsible for corrosion, while extensive discontinuous precipitation can be innocuous. This differs from the opinion of the eminent metallurgist Cyril Stanley Smith, who suggested that discontinuous precipitation makes grain boundaries highly susceptible to corrosion, /16/. However, the present results are consistent with the experience of Peter Northover, /17/, who observed intergranular corrosion and cracking in ancient Bactrian silver despite copper contents less than 1 %, which is almost certainly too low for discontinuous precipitation to occur, /2/.

Be that as it may, there is a possible link between retained cold-work and the occurrence of discontinuous precipitation. Cold-deformation can reduce the early growth rate of discontinuous precipitation in silver-copper alloys at elevated temperatures, and this could be due to deformation-induced continuous precipitation within the grains, /18/. A similar effect may have occurred in the Cauldron samples 361, 363 and 365, even to the extent that discontinuous precipitation was prevented. Verification of this would require Transmission Electron Microscopy (TEM) of thin foils prepared from small samples, which is technically possible using Focussed Ion Beam (FIB) or Dual Beam equipment.

An important aspect particularly relevant to restoration and conservation is illustrated by the Egyptian vase and the Byzantine paten. This is the effect of decorative chasing and stamping on the corrosion damage. The cracks along the chasing grooves in figure 2, the interpretation of figure 6, and the breakages along the circular grooves of the paten, suggest that all thin-walled objects with chased or stamped decorations should be examined for corrosion damage especially at the corresponding *internal* or *rear surface* locations. If this is so, a possible remedial measure is to apply a protective coating to these surfaces, /4/.

### 2.6 Survey of diagnostic techniques

Owing to its complexity, the embrittlement of ancient silver requires a number of diagnostic techniques for its assessment. Table 1 surveys these techniques, classified into four main topics:

- (1) *Visual inspection*: This is obvious, but nevertheless essential. Only visual inspection gives an overall impression of an object's condition. This should be photographically documented, with colour photography as an important option for corroded objects, e.g. /20/.
- (2) *X-ray radiography*: This can reveal both internal and external "hidden" damage and evidence of restorations. (It can also help to determine how a complex object is assembled, e.g. the Roman kantharos mentioned earlier, /21/.)
- (3) *Metallography, EBSD, EDX or WDX, microhardness*: Metallography is generally the most important diagnostic technique, especially when SEM is combined with EBSD and chemical analysis using EDX or WDX (Wavelength Dispersive analysis of X-rays). Microhardness testing coupled to SEM metallography can be very helpful in determining the types and severity of embrittlement, /1–2, 4/. Figure 15 gives an example.
- (4) *Fractography*: This is an essential adjunct to metallography for distinguishing between the types of embrittlement. Detailed fractography requires considerable interpretative skill, /2/.

### 2.7 Remedial measures

Extensive discussions of the remedial measures for restoration and conservation of embrittled ancient silver are provided in references /2–4/. A summary is given here:

- Detailed case histories are important - indeed essential - for determining the best ways to restore and conserve embrittled objects.
- The best remedial measures, from the point of view of preserving the objects, are not always reversible. This is a controversial topic!
- All remedies are mixtures of *pros* and *cons*: each case must be considered on its own merits and in the light of ethical considerations and current technical capabilities.

### 3. ROMAN PILE-SHOE EMBRITTLEMENT

Obstacles in the Maas riverbed near Cuijk, the Netherlands, were recognised in the early 1990s to be the remains of a Roman bridge. A recovery programme found and removed many stone blocks and the remains of more than 100 oak piles. Some of the pointed lower ends of the piles were still covered by iron pile-shoes. Each pile-shoe was made from four iron bars, joined by heating and hammer-welding to form a point. The piles, and hence the pile-shoes, were dated to between 340 AD and 400 AD, /22/.

The piles and attached pile-shoes were transported for storage in a large concrete-floored shed. One pile-shoe was found to have three broken bars with at least one recent fracture. This was an impact fracture caused by a fall to the floor of the shed. The pile-shoe was sent to the Museum Het Valkhof in Nijmegen, where a slice containing one of the recent fracture surfaces was sawn off.

Figure 16 is a detail of the pile-shoe, showing all three broken bars and the sawn-off slice, which included the upper fracture surface of the recent breakage. Figure 17 is a macrophotograph of the lower fracture surface. During the centuries in the river bed the bar had corroded non-uniformly to depths up to about 0.5 mm. The largely internal fracture consisted of shiny uncorroded facets, some of which were up to 3 mm in diameter. This unusual and obviously brittle fracture prompted a collaborative investigation using several diagnostic techniques.

#### 3.1 *The collaborative investigation*

The sawn-off slice shown in figure 16 was struck on a side surface with a hammer, resulting in brittle fracture into large fragments. This confirmed the ambient temperature impact brittleness of the bar at the location of the original breakage. The fragments were then used for the investigation surveyed in table 2. Choice of the diagnostic techniques developed as the investigation proceeded. For example, it became clear that fresh, uncontaminated fracture surfaces should be examined, if possible, for evidence of phosphorus segregation to grain boundaries. Unfortunately, specimens could not be made for *in vacuo* fracture and examination by Auger Electron Spectroscopy (AES). Instead, recourse was made to breaking a sample in a nominally inert atmosphere and interrogating the fracture surface by X-ray Photoelectron Spectroscopy (XPS). This was unsatisfactory and inconclusive, /6, 7/.

The results for the three main topics in table 2 are summarised here:

- (1) *Fractography*: Figure 18 shows FEG-SEM images of the brittle fracture, which was almost entirely intergranular at, and near, the outside surfaces, and a mixture of intergranular and cleavage fracture towards the centre of the bar. The grain size varied from 0.25 mm to more than 2 mm.
- (2) *Metallography*: Figure 19 shows a cross-section including the fracture surface. The three zones are the result of hot-welding three strips of iron together to form the bar. The microstructure consists of large undeformed ferrite grains, some deformation twinning close to the outside surfaces, and an unusual etching effect especially in zone 2. This effect is due to phosphorus segregation and typically occurs in ancient phosphoric iron, /23–24/.
- (3) *Chemical analyses*: These showed that the bar is a phosphoric iron (0.25–0.52 wt.% P) with very low silicon, manganese and sulphur contents; and extremely low carbon content (0.0033 wt.% C) at the location of the original breakage, /6–7/. The XRD analyses also showed that the surface corrosion layer was akaganeite, which would have formed after recovery of the pile-shoe from the riverbed, /6–7, 25/.

#### 3.2 *Embrittlement mechanisms*

Embrittlement of the bar was attributed to the *locally* extremely low carbon content in combination with the relatively high phosphorus content, /6–7/. The large ferrite grain sizes suggest that the low carbon content was due to local decarburisation during final manufacture of the pile-shoe, /26/. This low carbon content enabled high-temperature segregation of phosphorus to the grain boundaries, resulting in susceptibility to brittle impact fracture at ambient temperatures, /27–30/. A contributing factor to the brittleness could have been a notch effect owing to non-uniform corrosion penetrating into the bar.

### 3.3 Conservation of other pile-shoes

There are two aspects to conserving the other recovered pile-shoes. Firstly, these must be expected to have surface corrosion layers containing akaganeite. Since akaganeite is hygroscopic, corrosion will continue unless actively prevented by drying out the corrosion layers and either storing the pile-shoes in a low-humidity environment, /25/, or applying a protective (organic) coating. Secondly, some or many of these pile-shoes could have extremely low carbon contents at similar locations along the bars. Thus if any are to be removed from storage, and whether or not they are still attached to piles, they should be handled and transported with care to avoid breakages.

## 4. CONCLUDING REMARKS

This paper has shown that modern diagnostic techniques, especially in metallography and chemical analysis, have provided improved understanding of embrittlement in ancient silver objects and an explanation of embrittlement and corrosion of an iron pile-shoe from a Roman bridge. This knowledge can be used for suggesting and applying the optimum remedial measures for restoration and conservation of these and similarly embrittled objects.

## 5. ACKNOWLEDGEMENTS

Special thanks are owed to Peter Northover, Oxford University, Oxford; Peter Seinen, Philips Lighting BV, Eindhoven; Arjen Rijkenberg, Corus RD and T, IJmuiden; Ronny Meijers, Museum Het Valkhof, Nijmegen; and Tim Hattenberg, NLR, Emmeloord. Several other colleagues, not mentioned in the paper and references, also assisted in the investigations: Ron Leenheer, Allard Pierson Museum, Amsterdam; Bart Ankersmit and Ineke Joosten, Netherlands Institute for Cultural Heritage, Amsterdam; and Joanna Cook, The Menil Collection, Houston.

## 6. REFERENCES

1. Wanhill, R.J.H., Steijaert, J.P.H.M., Leenheer, R., Koens, J.F.W., Damage assessment and preservation of an Egyptian silver vase (300-200 BC), *Archaeometry*, 40 (1998), pp. 123-137.
2. Wanhill, R.J.H., Archaeological silver embrittlement: a metallurgical enquiry, NLR Technical Publication NLR-TP-2002-224, National Aerospace Laboratory NLR, Amsterdam, the Netherlands, 2002.
3. Wanhill, R.J.H., Embrittlement of ancient silver, *Journal of Failure Analysis and Prevention*, 5 (2005), pp. 41-54.
4. Wanhill, R.J.H., A lecture course on metallurgy, embrittlement and conservation of ancient silver, National Aerospace Laboratory NLR, Amsterdam, the Netherlands, 2008.
5. Wanhill, R.J.H., Embrittlement of ancient silver, Archaeometallurgy Application Note - EBSD & EDS, Ed. S. Wright, [www.edax.com](http://www.edax.com), 2008.
6. Wanhill, R.J.H., Seinen, P.A., Rijkenberg, R.A., Meijers, H.J.M., Investigation of a broken pile-shoe from a Roman bridge, *Historical Metallurgy*, 41, Part 1 (2007), pp. 32-39.
7. Wanhill, R.J.H., Seinen, P.A., Rijkenberg, R.A., Meijers, H.J.M., Investigation of a broken pile-shoe from a Roman bridge, NLR Technical Publication NLR-TP-2007-045, National Aerospace Laboratory NLR, Amsterdam, the Netherlands, 2007.
8. Thompson, F.C., Chatterjee, A.K., The age-embrittlement of silver coins, *Studies in Conservation*, 1 (1954), pp. 115-126.
9. Johnson, W., Mellor, P.B., Plasticity for Mechanical Engineers, D. van Nostrand Company Ltd., London, UK, 1962, pp. 333-334.
10. Northover, J.P., Personal communication, Department of Materials, Oxford University, Oxford, UK, 2003.

11. Wanhill, R.J.H., Northover, J.P., Hattenberg, T., On the significance of discontinuous precipitation of copper in ancient silver, NLR Technical Publication NLR-TP-2003-628, National Aerospace Laboratory NLR, Amsterdam, the Netherlands, 2003.
12. Wanhill, R.J.H., Hattenberg, T., Northover, J.P., Electron BackScatter Diffraction (EBSD) of corrosion, deformation and precipitation in the Gundestrup Cauldron, NLR Technical Publication NLR-TP-2003-490, National Aerospace Laboratory NLR, Amsterdam, the Netherlands, 2003.
13. Williams, D.B., Edington, J.W., The discontinuous precipitation reaction in dilute Al-Li alloys, *Acta Metallurgica*, 24 (1976), pp. 323-332.
14. W. Gust, Discontinuous precipitation in binary metallic systems, *in* Phase Transformations, The Institution of Metallurgists, London, UK, 1979, pp. II-27–II-68.
15. R.D. Doherty, Diffusive phase transformations in the solid state, *in* Physical Metallurgy, Eds. R.W. Cahn and P. Haasen, Elsevier Science B.V., Amsterdam, the Netherlands, 1996, Vol. II, pp. 1456-1458.
16. Smith, C.S., The interpretation of microstructures of metallic artifacts, *in* Application of Science in Examination of Works of Art, Ed. W.J. Young, Boston Museum of Fine Arts, Boston, USA, 1965, pp. 20-52.
17. Northover, J.P., Personal communication, Department of Materials, Oxford University, Oxford, UK, 1999.
18. Scharfenberger, W., Schmitt, G., Borchers, H., Über die Kinetik der diskontinuierlichen Ausscheidung der Silberlegierung mit 7,5 Gew.-%Cu, *Zeitschrift für Metallkunde*, 63 (1972), pp. 553-560.
19. Wanhill, R.J.H., Research in progress, National Aerospace Laboratory NLR, Emmeloord, the Netherlands, 2009.
20. Organ, R.M., The current status of the treatment of corroded metal artifacts, *in* Corrosion and Metal Artifacts, NBS Special Publication 479, National Bureau of Standards / U.S. Department of Commerce, Washington, D.C., USA, 1977, pp. 107-142.
21. Meijers, H.R.M, Personal communication, Museum Het Valkhof, Nijmegen, the Netherlands, 2007.
22. Haalebos, J.K., Goudswaard, B., Kroes, R.A.C., Beek, H. van der, De laat Romeinse tijd, *in* Cuijk, een Regionaal Centrum in de Romeinse Tijd, Editors H. Enkevort and J. Thijssen, Uitgeverij Matrijs, Utrecht, the Netherlands, 2002, pp. 80-95.
23. Stewart, J.W., Charles, J.A., Wallach, E.R., Iron-phosphorus-carbon system Part 3 – Metallography of low carbon iron-phosphorus alloys, *Materials Science and Technology*, 16 (2000), pp. 291-303.
24. Godfrey, E.G., Vizzaino, A., McDonnell, J.G., The role of phosphorus in early ironworking, *in* Prehistoric and Medieval Direct Iron Smelting in Scandinavia and Europe, Aspects of Technology and Society, Editor L.N. Nørbach, Aarhus University Press, Aarhus, Denmark, 2003, pp. 191-193.
25. Selwyn, L., Metals and Corrosion: A Handbook for the Conservation Professional, Canadian Conservation Institute, Ottawa, Canada, 2004.
26. Dinnetz, M.K., Technical and archaeological investigation of an early iron sword from Sweden, *in* Prehistoric and Medieval Direct Iron Smelting in Scandinavia and Europe, Aspects of Technology and Society, Editor L.N. Nørbach, Aarhus University Press, Aarhus, Denmark, 2003, pp. 101-109.
27. Inman, M.C., Tipler, H.R., Grain-boundary segregation of phosphorus in an iron-phosphorus alloy and the effect upon mechanical properties, *Acta Metallurgica*, 6 (1958), pp. 73-84.
28. Hopkins, B.E., Tipler, H.R., The effect of phosphorus on the tensile and notch-impact properties of high-purity iron and iron-carbon alloys, *Journal of the Iron and Steel Institute*, 188 (1958), pp. 218-237.
29. Ramasubramanian, P.V., Stein, D.F., An investigation of grain-boundary embrittlement in Fe-P, Fe-P-S, and Fe-Sb-S alloys, *Metallurgical Transactions*, 4 (1973), pp. 1735-1742.
30. Erhardt, H., Grabke, H.J., Equilibrium segregation of phosphorus at grain boundaries of Fe-P, Fe-C-P, Fe-Cr-P, and Fe-Cr-C-P alloys, *Metal Science*, 15 (1981), pp. 401-408.



Table 1 Diagnostic techniques for archaeological silver embrittlement, /2, 4/

<p><b>Visual Inspection (x1-x10) (unaided eye and hand lens)</b></p>	<p><b>X-ray Radiography (x1) (limited enlargement)</b></p>	<p><b>Optical (x10-x1000) and SEM (x10-x30,000) Metallography, EBSD, EDX or WDX, and Microhardness Testing (HV)</b></p>	<p><b>SEM Fractography (x10-x30,000)</b></p>
<p>Purpose: Object Basic Condition</p> <ul style="list-style-type: none"> <li>• nominally intact</li> <li>• restored</li> <li>• macrocrack patterns</li> <li>• missing pieces</li> <li>• fragmented</li> <li>• macrocrack patterns</li> <li>• missing pieces</li> </ul>	<p>Purpose: "Hidden" Damage</p> <ul style="list-style-type: none"> <li>• nominally intact, restored, or fragmented</li> <li>• hairline cracks</li> <li>• macrocracks</li> <li>• cracks following indented decorations</li> <li>• restored</li> <li>• missing pieces</li> </ul>	<p>Purpose: Manufactured Condition, Chemical Analysis, Internal Damage and Embrittlement</p> <ul style="list-style-type: none"> <li>• manufactured condition</li> <li>• mechanically worked } grain size, segregation bands, slip lines deformation and annealing twins</li> <li>• mechanically worked and annealed } coring, eutectic distribution</li> <li>• as-cast (dendritic)</li> <li>• cast and annealed</li> <li>• chemical analysis (SEM + EDX or WDX)</li> <li>• source: lead cupellation, native silver or aurian silver</li> <li>• lead, bismuth, antimony, tin, arsenic and thallium contents: linked to microstructurally-induced embrittlement</li> <li>• copper content             <ul style="list-style-type: none"> <li>- high purity (low copper) may be linked to retained cold-work</li> <li>- intentional additions of copper for strength</li> <li>- long-term discontinuous precipitation along grain boundaries</li> </ul> </li> <li>• corrosion-induced embrittlement (SEM + EBSD)</li> <li>• surficial</li> <li>• intergranular cracks: linked to cold-work or discontinuous precipitation of copper</li> <li>• interdendritic</li> <li>• transgranular corrosion along segregation bands,</li> <li>• transgranular corrosion and cracking linked to cold-work: slip lines, deformation twin boundaries, and slip-line fields below indented decorations</li> <li>• microstructurally-induced embrittlement             <ul style="list-style-type: none"> <li>• narrow intergranular cracks</li> <li>• bodily displaced grains</li> </ul> </li> <li>• microhardness testing (HV)             <ul style="list-style-type: none"> <li>• annealed } HV values also depend on chemistry, especially copper content</li> <li>• retained cold-work } HV values and possible nucleation of new cracks</li> <li>• corrosion } of new cracks</li> <li>• microstructural embrittlement</li> </ul> </li> </ul>	<p>Purpose: Embrittlement Types</p> <ul style="list-style-type: none"> <li>• corrosion-induced embrittlement</li> <li>• surficial corrosion</li> <li>• corroded fracture surfaces with fine granular appearance like surficial corrosion</li> <li>• transgranular fracture (crystallographic) along slip bands and deformation twin boundaries, possibly also along annealing twin boundaries</li> <li>• microstructural embrittlement             <ul style="list-style-type: none"> <li>• mainly clean grain boundary facets: can show local corrosion where slip lines, deformation twins and segregation bands intersect the fracture surfaces</li> <li>• narrow intergranular cracks</li> <li>• bodily displaced grains</li> </ul> </li> </ul>

Table 2 Diagnostic techniques for the pile-shoe embrittlement, /6, 7/

Techniques	Specific Aspects and Purposes	Organisation
Fractography <ul style="list-style-type: none"> <li>• Macrofractography</li> <li>• SEM / FEG-SEM</li> </ul>	brittle fracture, corrosion intergranular + cleavage fracture	Het Valkhof PR-MA / NLR
Optical metallography	microstructure, hardness	CORUS, NLR
Chemical analysis <i>Bulk</i> X-Ray Diffraction (XRD) X-Ray Fluorescence (XRF) spectroscopy Combustion + InfraRed (IR) detection	iron and surface corrosion layer iron composition carbon and sulphur content of iron	PR-MA CORUS CORUS
<i>Metallographic surfaces</i> SEM+EDX, Electron Probe MicroAnalysis (EPMA)+WDX	iron and inclusion compositions, phosphorus and oxygen line scans	CORUS / PR-MA
<i>Fracture surfaces</i> X-rayPhotoelectron Spectroscopy (XPS)	grain boundary segregation	PR-MA

Het Valkhof = Museum Het Valkhof, Nijmegen; PR-MA = Philips Research-Materials Analysis, Eindhoven; CORUS = Corus Research, Development and Technology, IJmuiden

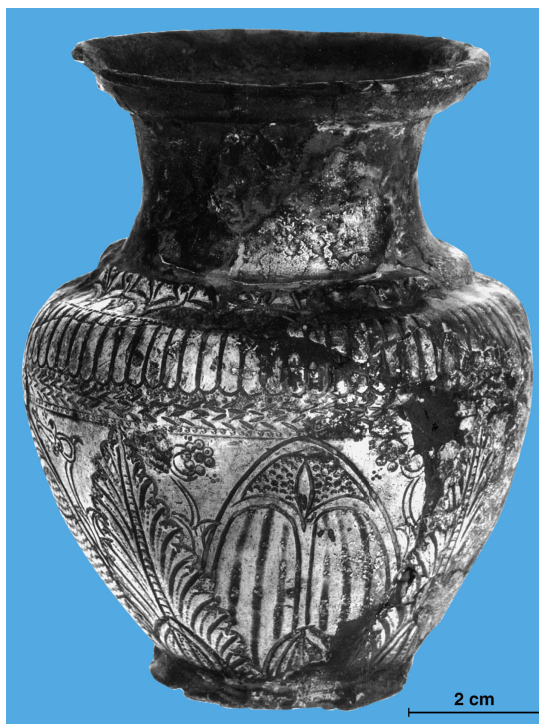


*Fig. 1 The Egyptian vase*



*Fig. 2 X-ray radiograph of the Egyptian vase:  
hairline cracks A follow external chasing grooves*

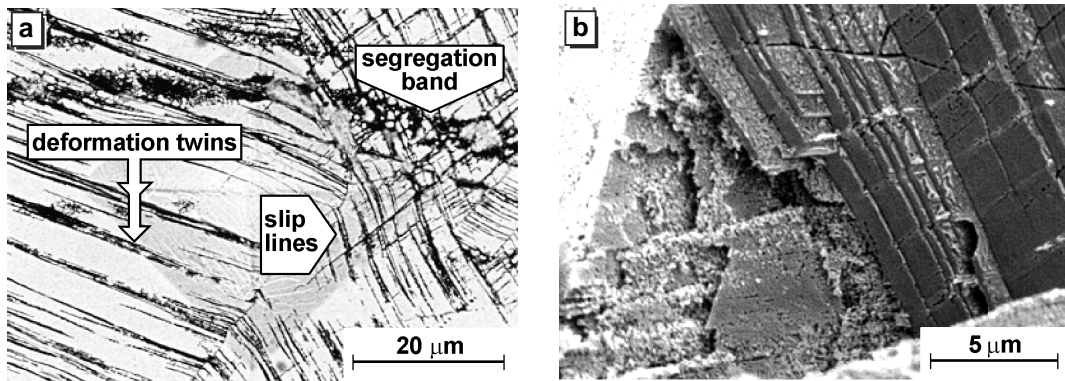


Fig. 3 Examples of corrosion-induced embrittlement in the Egyptian vase: (a) corrosion along slip lines, deformation twin boundaries and segregation bands, and (b) crystallographic fracture due to corrosion along slip lines and deformation twins: SEM metallograph and fractograph

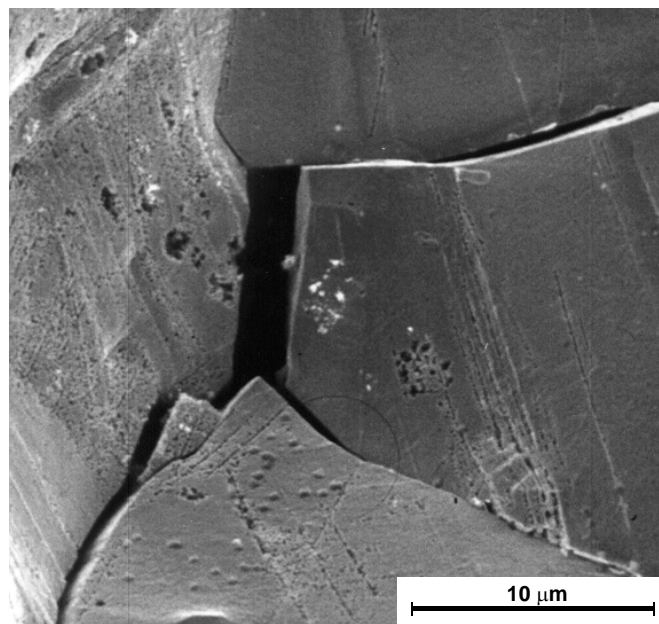


Fig. 4 Microstructurally-induced brittle intergranular fracture in the Egyptian vase: SEM fractograph

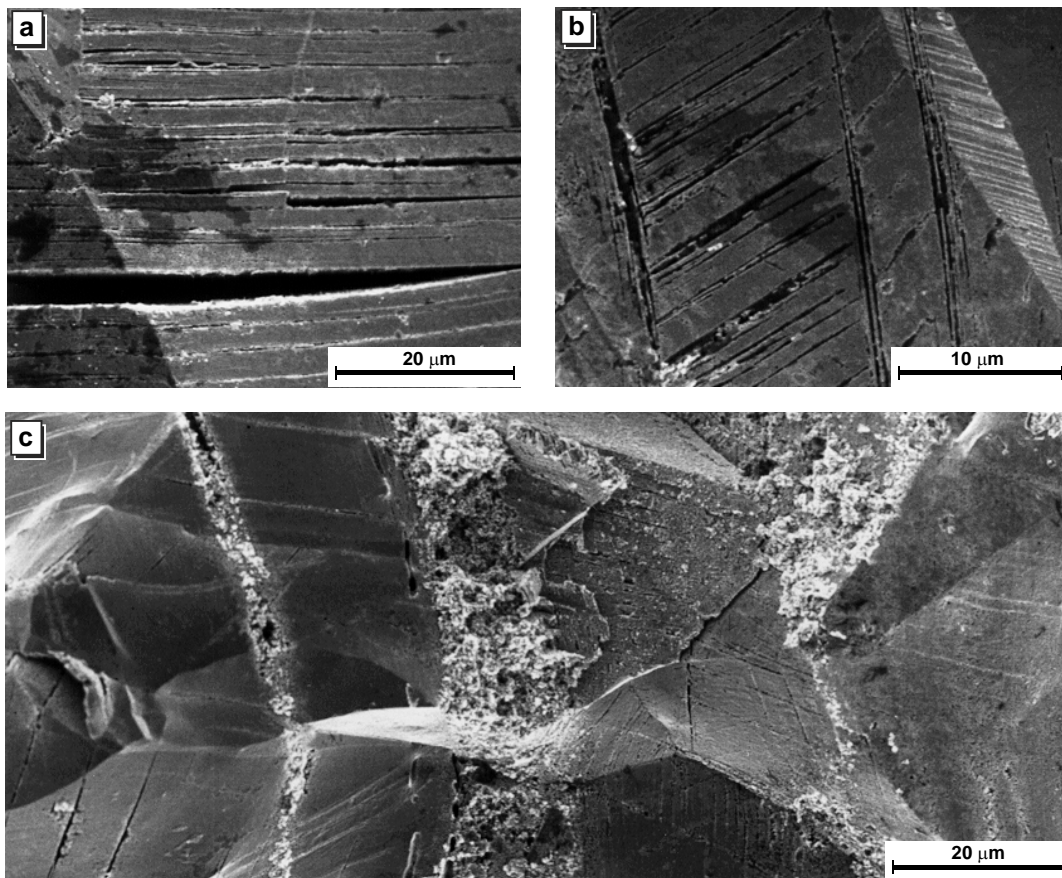


Fig. 5 Examples of synergistic embrittlement in the Egyptian vase: (a) corrosion (causing fracture) along slip lines intersecting grain boundary facets, (b) corrosion along deformation twin boundaries intersecting a grain boundary, and (c) corrosion along segregation bands intersecting grain boundary facets: SEM fractographs

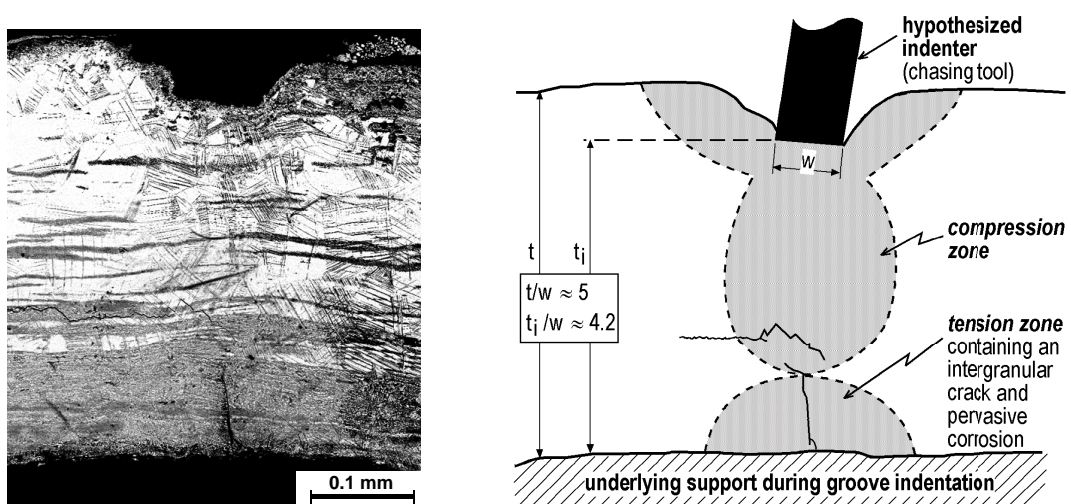


Fig. 6 Through-thickness BackScattered Electron (BSE) metallograph and schematic of an external chased decorating groove in the Egyptian vase. The sample is from the vase lower wall



Fig. 7 The Gundestrup Cauldron

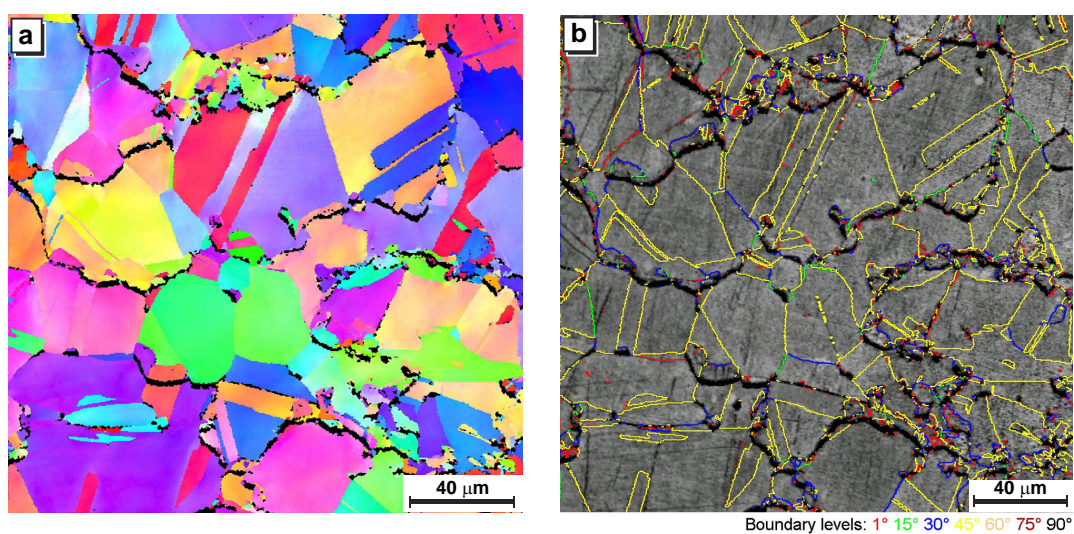


Fig. 8 IPF colour-coded map and boundary rotation angle map for Gundestrup Cauldron sample 366. The yellow-coded boundaries are mainly annealing twins

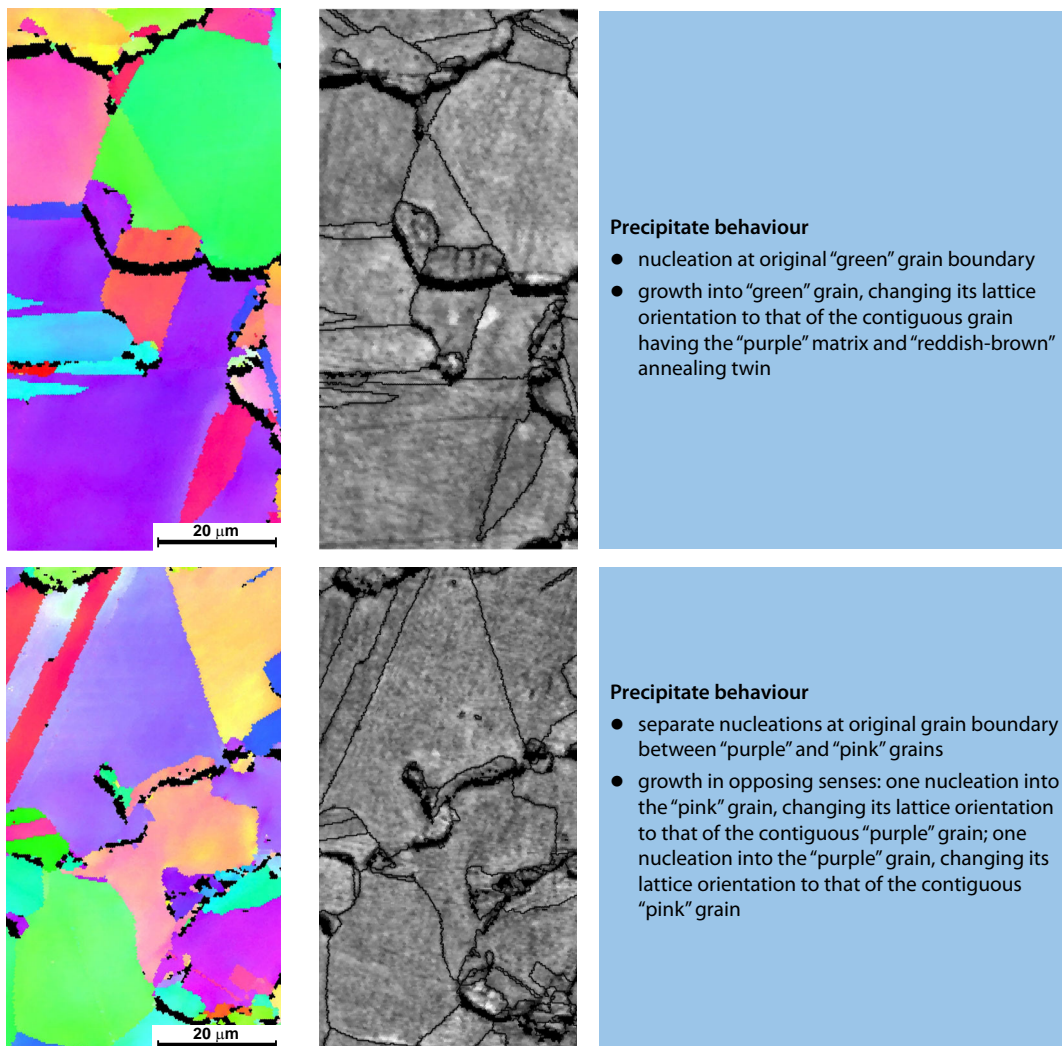


Fig. 9 Details of precipitate nucleation and growth in Gundestrup Cauldron sample 366

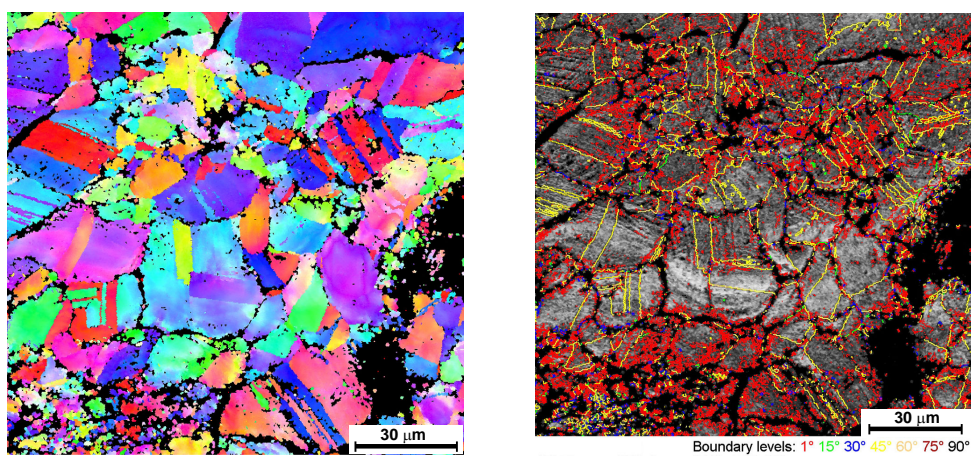


Fig. 10 IPF colour-coded map and boundary rotation angle map for Gundestrup Cauldron sample 361

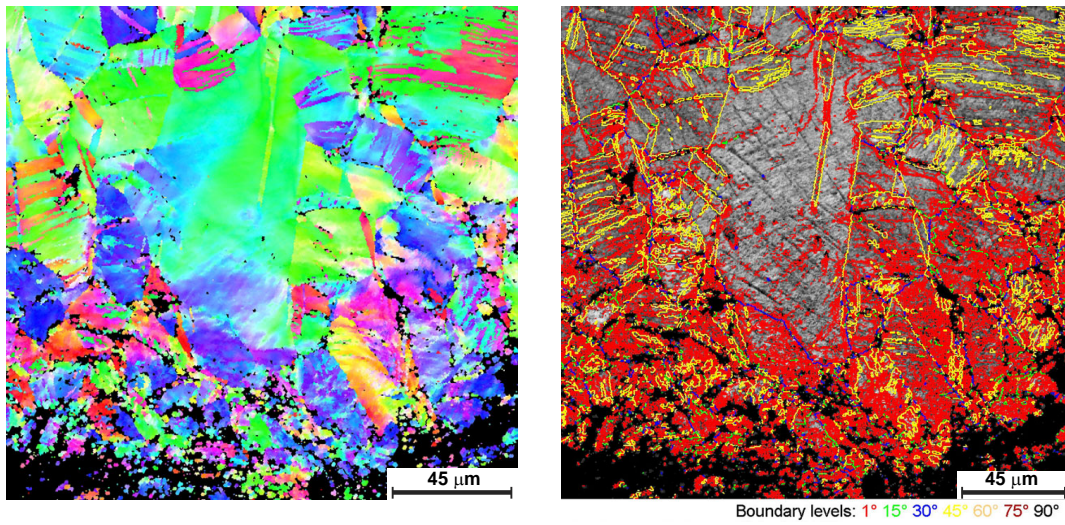


Fig. 11 IPF colour-coded map and boundary rotation angle map for Gundestrup Cauldron sample 363

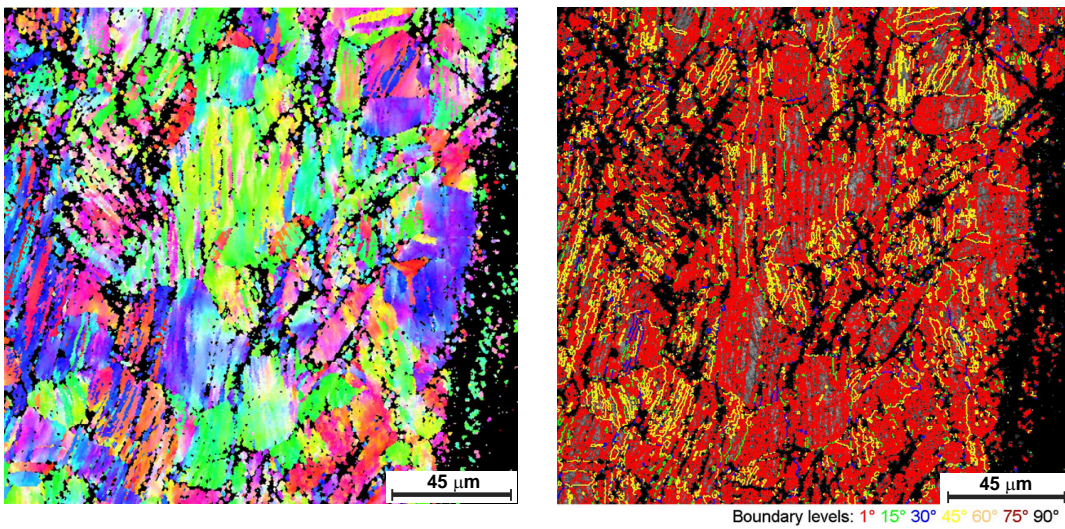


Fig. 12 IPF colour-coded map and boundary rotation angle map for Gundestrup Cauldron sample 365



Fig. 13 *The Byzantine paten: photograph courtesy of The Menil Collection, Houston*

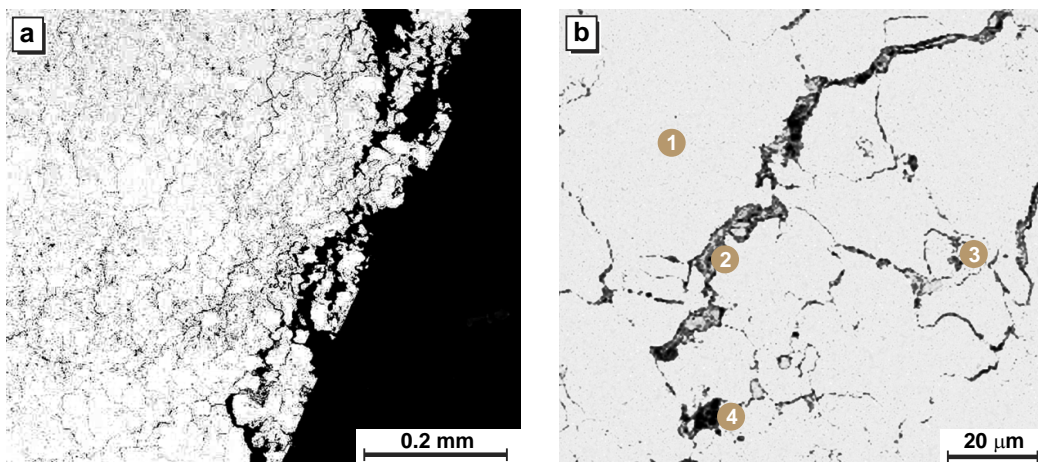
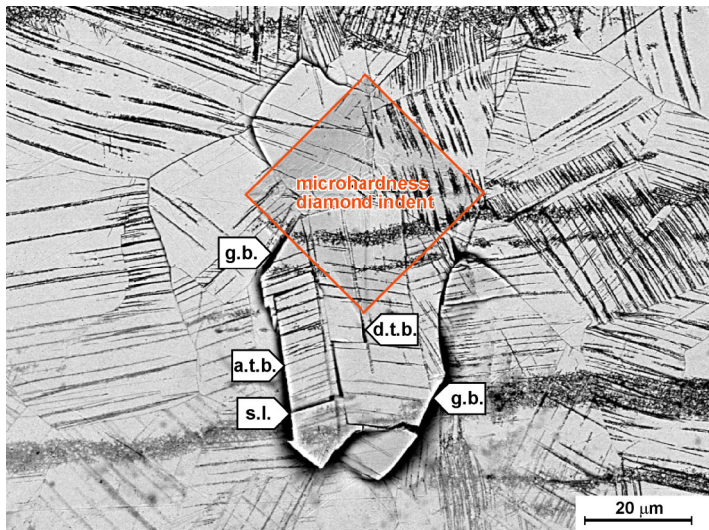


Fig. 14 *Examples of (a) intergranular corrosion and (b) discontinuous precipitation of copper at grain boundaries in the Byzantine paten. EDX analyses showed primarily silver at location 1, and silver and copper at locations 2-4: SEM metallographs and analyses courtesy of Ineke Joosten, ICN*



**Key**

- b.g. : grain boundary crack
- s.l. : slip line crack
- d.t.b. : deformation twin boundary crack
- a.t.b. : annealing twin boundary crack

Fig. 15 Example of microhardness test for silver brittleness: Egyptian vase, SEM metallograph

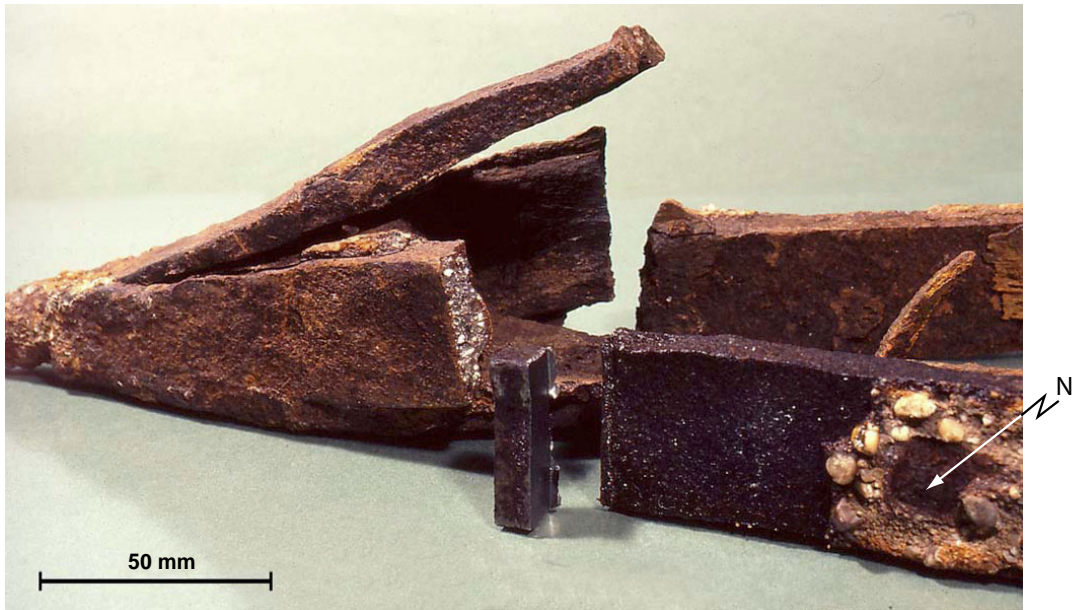


*Fig. 16 The broken pile-shoe with a sawn-off slice containing the upper fracture surface of the recent break. "N" indicates the head of a nail driven through a hole in the bar in order to attach it to the wooden pile*

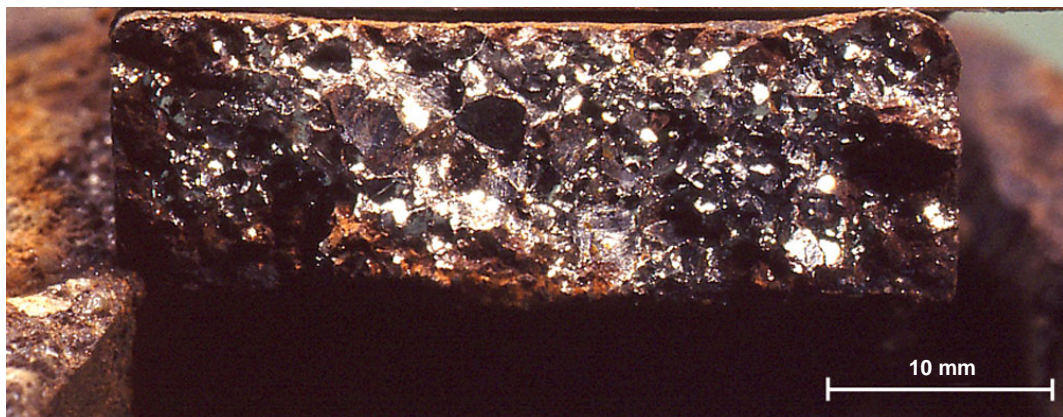


*Fig. 17 The lower fracture surface of the recent break*

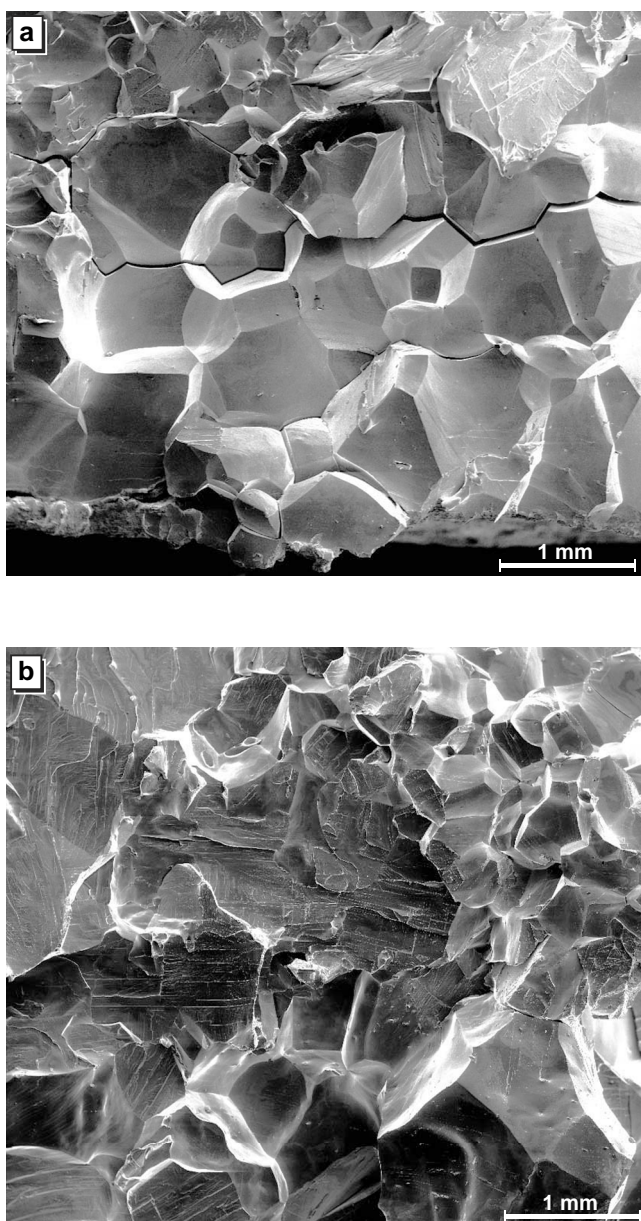


*Fig. 18 FEG-SEM fractographs of a sample from the sawn-off slice: (a) at, and near, the external surface, (b) nearer the centre*

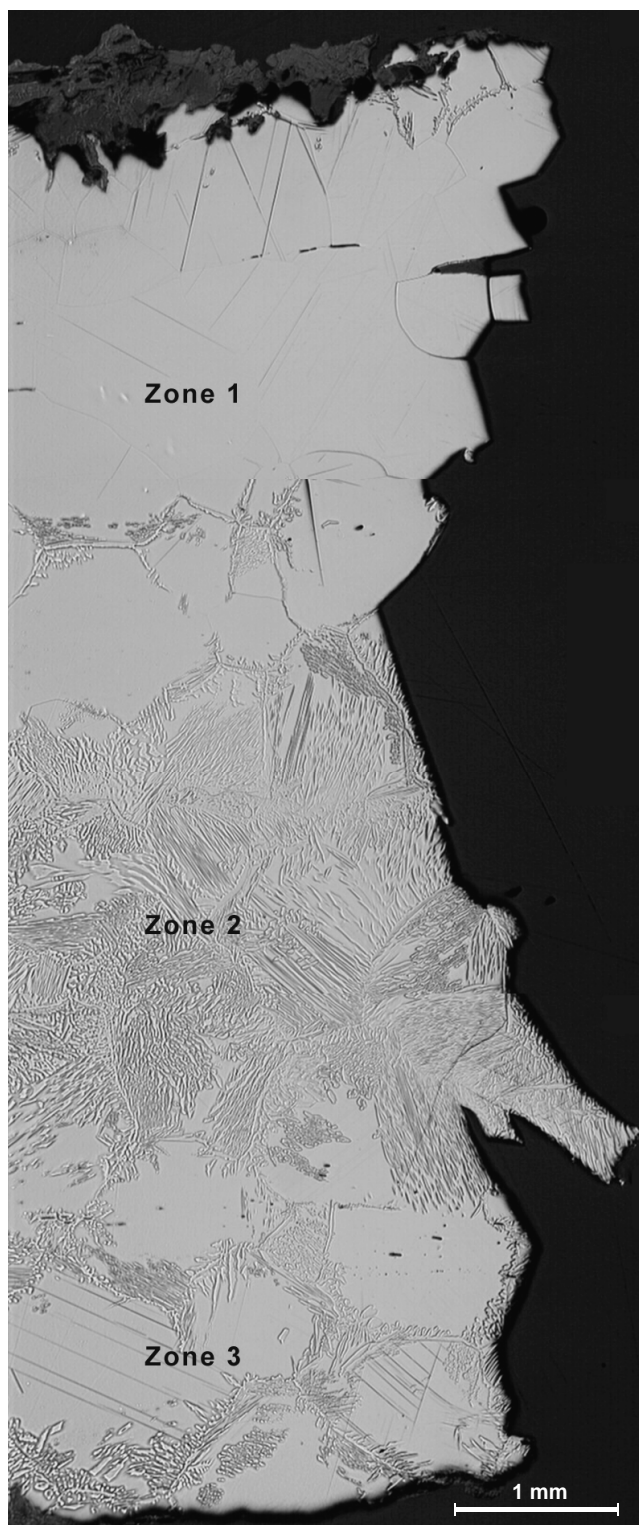


*Fig. 19 Through-thickness microstructure of a broken sample: the top and bottom edges are the original surfaces: SEM metallograph*